New Approaches for Birefringence Tuning in Vertical-Cavity Surface-Emitting Lasers

Tobias Pusch

Using the elasto-optic effect we increase the frequency difference between the two orthogonally polarized modes, the so-called birefringence splitting, in standard single-mode oxide-confined GaAs-based vertical-cavity surface-emitting lasers (VCSELs). The birefringence may play an important role in the realization of ultrafast polarization modulation for high-speed data transmission. For practical implementation it is necessary to miniaturize the strain-inducing mechanism for birefringence tuning in VCSELs. The goal is the realization of integrated structures on the VCSEL chip. In this article we discuss our work on miniaturized bending devices as the next step in achieving extremely high birefringence splitting. Furthermore measurements with integrated hotspot structures on VCSEL chips were made to reach much smaller scales for birefringence fine-tuning.

1. Introduction

VCSELs are extensively used today as transmitters in high-speed optical interconnects. A first generation of 25 to 28 Gbit/s devices is currently being deployed. Although digital modulation at about 71 Gbit/s with transmitter equalization has been shown [1], it is not certain that 100 Gbit/s signals can be generated by direct current modulation. A potential alternative to direct intensity modulation might be found in the research on birefringence splitting, i.e., the frequency difference between the two orthogonally polarized components of a VCSEL mode. It has been demonstrated that by optical spin injection a birefringent VCSEL can be excited to oscillations in the degree of circular polarization [2]. Here the oscillation frequency is nearly equal to the birefringence splitting. The generation of extremely fast polarization bursts was shown as well [2]. Contributions to the birefringence are geometrical anisotropies, the electro-optic effect in the cavity, and incorporated strain [3]. Mechanically induced strain seems to be the most promising way. We have achieved a record-high birefringence splitting of more than 250 GHz via direct substrate bending [4]. As a next step, new miniaturized concepts for birefringence tuning have to be investigated.

2. Options for Miniaturized Mechanical Strain Incorporation

The maximum birefringence splitting of 259 GHz [4] has been reached by bending a $10 \times 10\,\mathrm{mm}^2$ large VCSEL sample with the custom-made mount sketched in Fig. 1. The aim was to reach birefringence splittings of more than 100 GHz. We have found that values of 100–150 GHz are safely obtainable without sample failure. Based on this result, a much

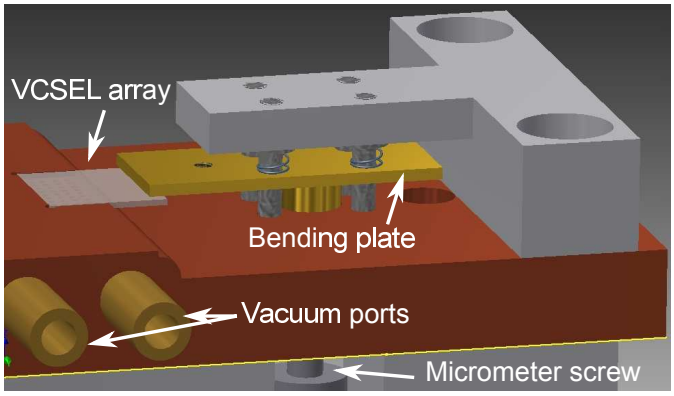

Fig. 1: Drawing of our first custom-made mount with bending plate and VCSEL array sample [4].

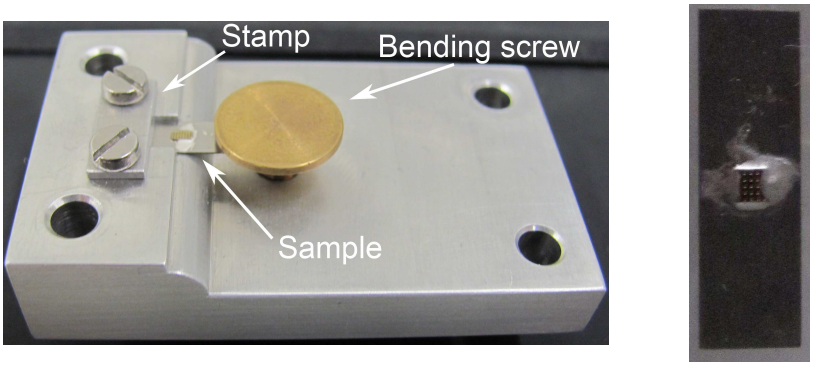

Fig. 2: Miniaturized second-generation bending device. A metal stripe with a glued VCSEL array is fixed in a recess via a stamp. Strain is induced indirectly in the VCSEL array by bending the free part of the metal stripe by movements of the screw (left). The VCSEL array is mounted with conductive glue on the $10 \times 4\,\mathrm{mm}^2$ large metal stripe (right).

simpler miniaturized bending mount can be constructed. It is depicted in Fig. 2, together with a mounted sample.

In contrast to the mount in Fig. 1 we use indirect bending. The VCSEL array with a size of $1 \times 1\,\mathrm{mm}^2$ is 100 times smaller than in the first bending device. The array is fixed on a metal stripe via conductive glue. The stripe itself is fixed on the left side by a stamp (see Fig. 2, left) and about half the area is free-standing. The position of the VCSEL array is close to the edge of the recess to achieve a maximum effect. We use a screw with a pitch of 350 µm to bend the metal stripe and thereby to induce strain indirectly in the VCSEL sample. The resulting optical spectrum for large bending is shown in Fig. 3 (left). With a value of 226 GHz we have reached a comparably high birefringence splitting as with the first bending device. The measurement was stopped here in order not to risk sample damage. Figure 3 (right) displays the light–current–voltage (LIV) curves of the investigated standard single-mode oxide-confined VCSEL with about 4 µm active diameter. The threshold current and voltage are 0.44 mA and 1.82 V, respectively. An optical output power of 1.0 mW is reached at about $I = 1.82\,\mathrm{mA}$ current. The higher-order transverse mode is still suppressed by approximately 25 dB at $I = 2.1\,\mathrm{mA}$.

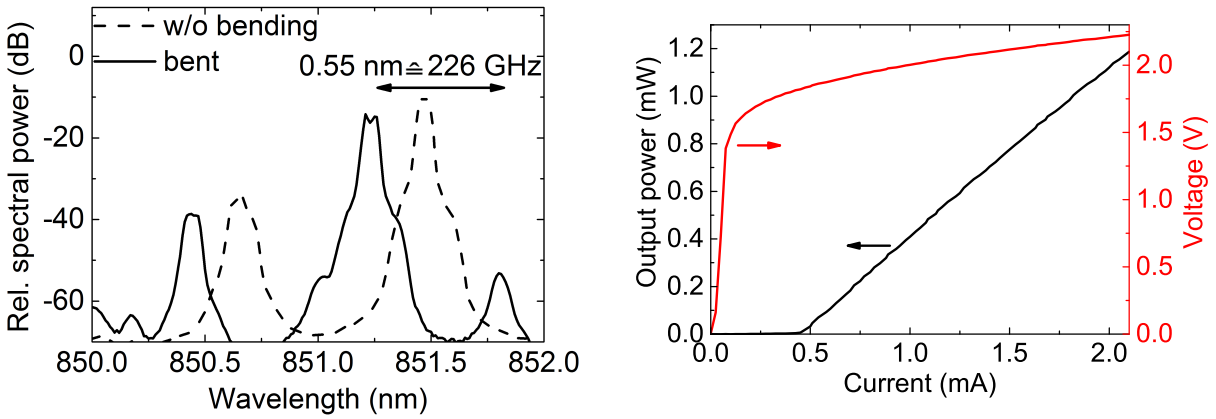

Fig. 3: Optical spectra without bending and with maximum applied bending of the metal stripe, measured at 2.1 mA (left). LIV characteristics at maximum bending (right).

3. Approaches to Thermal Birefringence Tuning

The ultimate miniaturization step is a birefringence tuning mechanism integrated on the VCSEL chip. At this level, mechanical bending seems impractical. Mechanisms for thermally induced strain are more simple to construct. Studies with an external heat source were made by Jansen van Doorn et al. [5, 6] for birefringence tuning in VCSELs. In this case a Ti-sapphire laser beam was focused close to the VCSEL and the induced heat deformed the crystal structure. The change of birefringence (less than 3 GHz reversible [5] and 23 GHz with material ablation [6]) is substantially smaller compared to mechanical bending due to the much lower induced stress.

We have made alternative investigations using standard 850 nm oxide-confined single-mode VCSEL samples from Philips Technologie GmbH (U-L-M Photonics) which were partly post-processed. The first sample design comprises three VCSELs per unit cell, where one of them is a regular VCSEL structure. The other two are metalized on the surface and can be used as hotspots. We measure the optical spectra and the LIV curves for different current flow in one of the metalized VCSELs. The current in the lasing VCSEL is constant at $I = 2.1\,\mathrm{mA}$. A photograph of the device and measured optical spectra for different tuning currents are depicted in Fig. 4. The spectra show a red-shift of the fundamental mode as a result of a temperature increase in the lasing VCSEL. However, no increase of the birefringence splitting is seen. With an estimated wavelength shift rate of 0.07 nm/K [7] we get a temperature increase in the lasing VCSEL of about $\Delta T = 2.4\,\mathrm{K}$. The main problem is visible in Fig. 4 (left). The distance of 75 µm between the lasing VCSEL and the heat-inducing metalized VCSEL is simply too large. In other words, the thermal cross-resistance $R_{\mathrm{Th,X}} = \Delta T / P_{\mathrm{diss}} = 2.4\,\mathrm{K}/(3.51\,\mathrm{V} \cdot 10\,\mathrm{mA}) = 0.068\,\mathrm{K/mW}$ is very low owing to a thick (thermally insulating) polyimide layer employed for sample planarization. We get a slightly improved result of $\Delta T = 2.9\,\mathrm{K}$ from a second measurement with the nearest-neighbor (68 µm distance) VCSEL of Fig. 4 (left).

The second investigated sample has been post-processed in the cleanroom. We have placed a 120 nm thick nickel line in the vicinity of the VCSEL to potentially increase the thermal cross-resistance. As in the first case of Fig. 4 we have measured the LIV curves and

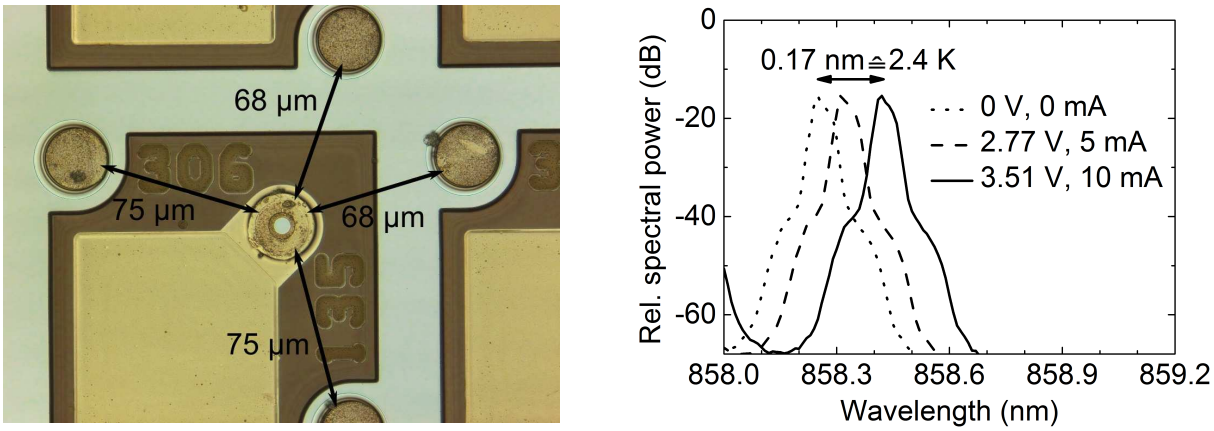

Fig. 4: Photograph of a sample with three VCSELs per unit cell. The distances between the lasing VCSEL and the metalized heating VCSELs are indicated (left). Optical spectra for different heating currents in a 75 µm distance metalized VCSEL (right).

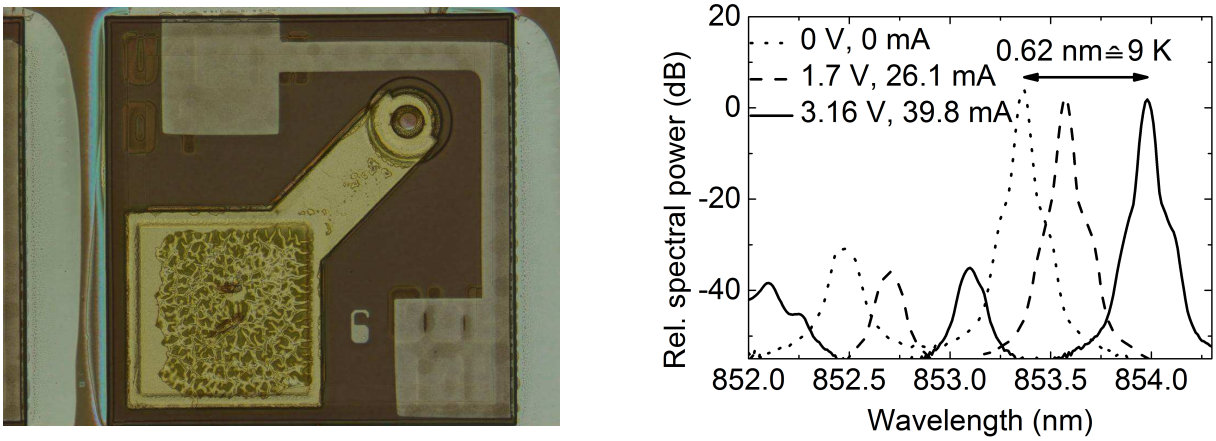

Fig. 5: Post-processed VCSEL sample with a nickel heating line (left). Optical spectra for different heating currents are shown on the right.

optical spectra for different currents in the nickel line. A photograph of the sample and measured optical spectra are shown in Fig. 5. The laser current is $I = 2.5\,\mathrm{mA}$. Every unit cell is surrounded by large trenches. For that reason it was not possible to run a straight heating line across unit cells. Instead, the line and both bondpads had to be confined in one unit cell, which resulted in a non-ideal geometry of a 90° bent heating line. To get the main heating on one side we adjust the distance of the nickel line to the VCSEL. In Fig. 5 the horizontal line is closer to the VCSEL and should have a larger heating effect. In the optical spectra in Fig. 5, a red-shift is clearly seen. With a wavelength shift rate of 0.07 nm/K we get a temperature increase of about $\Delta T = 9\,\mathrm{K}$ but no measurable increase of the birefringence splitting. The thermal cross-resistance with a value of $R_{\mathrm{Th,X}} = 9\,\mathrm{K}/(3.16\,\mathrm{V} \cdot 39.8\,\mathrm{mA}) = 0.072\,\mathrm{K/mW}$ is insignificantly larger than in the previous hotspot design.

The obtained results make clear that the small temperature increase (and temperature gradient) in the active VCSEL originates in the bad thermal conductivity between the

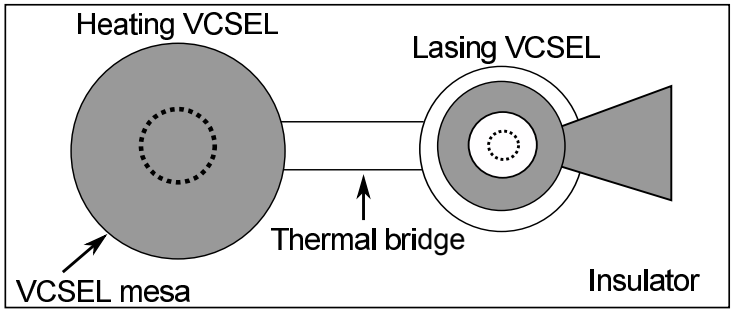

Fig. 6: Schematic top view of a VCSEL chip design for thermal tuning. Dark color and the dashed lines indicate deposited metal and the oxide apertures, respectively.

heating element and the VCSEL. To solve this problem, a revised VCSEL design is necessary. As a possible candidate we investigate the structure sketched in Fig. 6, which incorporates a thermal bridge between the heating element and the active VCSEL.

For convenience, the heat is again generated by a VCSEL with a metalized surface. In the previous designs of Figs. 4 and 5, a polyimide layer (necessary for planarization and electrical insulation) on the surface of the VCSEL chip has led to low lateral thermal conductivity. For the thermal bridge in the new design a compromise must be found between good thermal conductivity and electrical insulation. Thermal simulations are underway to identify, among others, the influence of thermal bridge dimensions (width, length, height) on achievable thermal cross-resistances and stress gradients.

4. Conclusion

New approaches for birefringence tuning in VCSELs were shown. With a second-generation bending device we have obtained a birefringence splitting up to 226 GHz by indirect bending with much smaller sizes of the mount and the sample. Further investigations into thermally induced strain were made. Measurements with integrated hotspot structures show only an internal heating of the VCSEL but no visible increase of the birefringence splitting. Custom-made VCSEL chip designs with optimized placement of heating elements have to be implemented. First simulations are in progress.

5. Acknowledgment

The author thanks Rudolf Rösch and Willi Kogler for fruitful discussions and technical support. Furthermore the author is grateful to Philips Technologie GmbH (U-L-M Photonics) for the provision of the VCSEL samples. This work is funded by the German Research Foundation.

References

[1] D.M. Kuchta, A.V. Rylyakov, F.E. Doany, C.L. Schow, J.E. Proesel, C.W. Baks, P. Westbergh, J.S. Gustavsson, and A. Larsson, "A 71-Gb/s NRZ modulated 850-nm VCSEL-based optical link", *IEEE Photon. Technol. Lett.*, vol. 27, pp. 577–580, 2015.

[2] N.C. Gerhardt and M. Hofmann, "Spin-controlled vertical-cavity surface-emitting lasers", *Advances in Optical Technol.*, vol. 2012, pp. 268949-1–15, 2012.

[3] K. Panajotov and F. Prati, "Polarization Dynamics of VCSELs", Chap. 6 in *VCSELs*, R. Michalzik (Ed.), pp. 181–231. Berlin: Springer, 2013.

[4] T. Pusch, M. Lindemann, N.C. Gerhardt, M.R. Hofmann, and R. Michalzik "Vertical-cavity surface-emitting lasers with birefringence splitting above 250 GHz", *Electron. Lett.*, vol. 51, pp. 1600–1602, 2015.

[5] A.K. Jansen van Doorn, M.P. van Exter, and J.P. Woerdman, "Elasto-optic anisotropy and polarization orientation of vertical-cavity surface-emitting semiconductor lasers", *Appl. Phys. Lett.*, vol. 69, pp. 1041–1043, 1996.

[6] A.K. Jansen van Doorn, M.P. van Exter, and J.P. Woerdman, "Tailoring the birefringence in a vertical-cavity semiconductor laser", *Appl. Phys. Lett.*, vol. 69, pp. 3635–3637, 1996.

[7] R. Michalzik, "VCSEL Fundamentals", Chap. 2 in *VCSELs*, R. Michalzik (Ed.), pp. 19–76. Berlin: Springer, 2013.